An autoinhibitory control element defines calcium-regulated isoforms of nitric oxide synthase.

John C. Salerno[1], Dawn E. Harris[1] , Kris Irizarry[1], Binesh Patel[1], Arturo J. Morales[1], Susan M.E. Smith[2], Pavel Martasek[3], Linda J. Roman[3], Bettie Sue S. Masters[3], Caroline L. Jones[4,*], Ben A. Weissman[4], Paul Lane[4], Qing Liu[4,5], and Steven S. Gross[4,5]

1 Department of Biology, Rensselaer Polytechnic Institute
2 Aeneas Biotechnology, Troy, New York 12180
3 Department of Biochemistry, The University of Texas Health Science Center, San Antonio, Texas 78284-7760
4 Department of Pharmacology, Cornell University Medical College, New York, New York 10021
5 Program in Biochemistry and Structural Biology, The Cornell University Graduate School of Medical Sciences, New York, New York 10021
* C.L. Jones is now C.L. Smith and works within the School of Biosciences

This is an electronic version of an article published in Journal of Biological Chemistry, 272 (47). pp. 29769-29777, November 1997. Journal of Biological Chemistry is available online at:

http://www.jbc.org/cgi/reprint/272/47/29769

THE JOURNAL OF BIOLOGICAL CHEMISTRY
Vol. 272, No. 47, Issue of November 21, pp. 29769–29777, 1997
Printed in U.S.A.

An Autoinhibitory Control Element Defines Calcium-regulated Isoforms of Nitric Oxide Synthase*

(Received for publication, March 31, 1997, and in revised form, August 25, 1997)

John C. Salerno‡, Dawn E. Harris‡§, Kris Irizarry‡, Binesh Patel‡, Arturo J. Morales‡, Susan M. E. Smith¶, Pavel Martasek‖, Linda J. Roman‖, Bettie Sue S. Masters‖, Caroline L. Jones, Ben A. Weissman**, Paul Lane**, Qing Liu§**‡‡, and Steven S. Gross**‡‡§§**

*From the ‡Department of Biology, Rensselaer Polytechnic Institute and ¶Aeneas Biotechnology, Troy, New York 12180, ‖Department of Biochemistry, The University of Texas Health Science Center, San Antonio, Texas 78284-7760, **Department of Pharmacology, Cornell University Medical College, New York, New York 10021, and ‡‡Program in Biochemistry and Structural Biology, The Cornell University Graduate School of Medical Sciences, New York, New York 10021*

Nitric oxide synthases (NOSs) are classified functionally, based on whether calmodulin binding is Ca^{2+}-dependent (cNOS) or Ca^{2+}-independent (iNOS). This key dichotomy has not been defined at the molecular level. Here we show that cNOS isoforms contain a unique polypeptide insert in their FMN binding domains which is not shared with iNOS or other related flavoproteins. Previously identified autoinhibitory domains in calmodulin-regulated enzymes raise the possibility that the polypeptide insert is the autoinhibitory domain of cNOSs. Consistent with this possibility, three-dimensional molecular modeling suggested that the insert originates from a site immediately adjacent to the calmodulin binding sequence. Synthetic peptides derived from the 45-amino acid insert of endothelial NOS were found to potently inhibit binding of calmodulin and activation of cNOS isoforms. This inhibition was associated with peptide binding to NOS, rather than free calmodulin, and inhibition could be reversed by increasing calmodulin concentration. In contrast, insert-derived peptides did not interfere with the arginine site of cNOS, as assessed from [^{3}H]N^G-nitro-L-arginine binding, nor did they potently effect iNOS activity. Limited proteolysis studies showed that calmodulin's ability to gate electron flow through cNOSs is associated with displacement of the insert polypeptide; this is the first specific calmodulin-induced change in NOS conformation to be identified. Together, our findings strongly suggest that the insert is an autoinhibitory control element, docking with a site on cNOSs which impedes calmodulin binding and enzymatic activation. The autoinhibitory control element molecularly defines cNOSs and offers a unique target for developing novel NOS activators and inhibitors.

Nitric oxide is a ubiquitous cell-signaling molecule, with protean roles in physiology and pathophysiology (1–3). Encoded by distinct genes, mammalian NO synthases (NOSs)[1] comprise a family of three calmodulin-dependent biopterohemoflavoproteins that are functionally distinguished by their modes of regulation (4). The two constitutively expressed isoforms of NOS (cNOSs), first identified in neuronal cells (nNOS) and endothelial cells (eNOS), remain dormant until calcium/calmodulin (Ca^{2+}/CaM) binding is actuated by transient elevations in intracellular Ca^{2+}. This Ca^{2+}-dependent mode of regulation provides pulses of NO for moment-to-moment modulation of vascular tone and neurosignaling. In contrast, activity of the immunostimulant-induced isoform of NOS (iNOS) is Ca^{2+}-independent, providing continuous high output NO generation for host defense. A remarkably high affinity for CaM, even at basally low levels of intracellular calcium, is responsible for the Ca^{2+} independence of iNOS (5).

Whether a given NOS isoform binds CaM in a Ca^{2+}-dependent or -independent manner has been assumed to be a property solely of the amino acid sequence specified by a 20–25-amino acid CaM binding site. However, this restrictive view is challenged by findings that chimeric eNOS and nNOS, which have had their CaM binding sequences replaced with the corresponding sequence from iNOS, still require Ca^{2+} for full activity (6, 7). Because regulation of enzyme systems by Ca^{2+}/CaM typically involves displacement of an intrinsic autoinhibitory polypeptide (8, 9), we hypothesized that the binding of Ca^{2+}/CaM to cNOSs may similarly trigger activation by displacing a control element. Here we identify a multiple amino acid insertion which serves as a control element unique to cNOSs and which molecularly defines Ca^{2+}-dependent isoforms of NOS.

EXPERIMENTAL PROCEDURES

Protein Modeling—Molecular modeling of the FMN binding module of nitric oxide synthase isoforms was done using the Insight and Homology programs from Biosym (BIOSYM/Molecular Simulations, San Diego, CA) running on a silicon graphics Indigo2 workstation. After alignment of NOS sequences with homologous FMN binding proteins of known structure (see "Results"), structurally conserved region (SCR) boxes were created corresponding to conserved regions of secondary structure and regions involved directly in FMN binding. These regions were characterized by high positive scores as evaluated by Dayhoff's mutation matrix (10). After assignment of coordinates in the SCR regions, the loop regions between the SCR boxes were modeled by searching the Brookhaven protein data base. The crude model structure was relaxed to a sterically and energetically reasonable state using the Discover program (BIOSYM/Molecular Simulations) for molecular me-

* This work was supported in part by National Institutes of Health Grants HL 50656 and HL 44603 (to S. S. G.), HL 30050 and GM52419 (to B. S. S. M.), and a grant from the Robert A. Welch Foundation (to B. S. S. M.). The costs of publication of this article were defrayed in part by the payment of page charges. This article must therefore be hereby marked "*advertisement*" in accordance with 18 U.S.C. Section 1734 solely to indicate this fact.

§ These authors contributed equally to the work.

§§ To whom correspondence should be addressed: Dept. of Pharmacology, Cornell University Medical College, 1300 York Ave., New York, NY 10021. Tel.: 212-746-6257; Fax: 212-746-8835; E-mail: ssgross@med.cornell.edu.

[1] The abbreviations used are: NOS, nitric oxide synthase; cNOS, calcium-dependent NOS, iNOS, calcium-independent NOS; eNOS, the endothelial isoform of cNOS; nNOS, the neuronal isoform of cNOS; CaM, calmodulin, SCR, structurally conserved region; CPR, cytochrome P450 reductase; DTT, dithiothreitol.

chanics and dynamics calculations. This includes splice repair to remove unrealistic structural features at SCR-loop junctions, end repair to assign reasonable structures to C-terminal and N-terminal extensions, and structural optimization to remove steric overlaps and to reduce the structure to a energetic minimum. Energy minimizations were begun using the steepest descent method; this was replaced by conjugate gradient method as convergence was approached.

Purification of NOS Isoforms—Rat neuronal cNOS (nNOS) and bovine endothelial cNOS (eNOS) were purified from *Escherichia coli* harboring pGroELS and pCW vector expression systems for nNOS and eNOS, as described previously (11, 12). iNOS-rich cytosol was prepared from rat aortic smooth muscle cells, which were isolated from Fisher rat thoracic aortae (13) and grown in 75-cm^2 culture flasks at passage 10–15. Cells were stimulated for 16 h in culture medium containing a combination of lipopolysaccharide (30 μg/ml) and rat recombinant interferon-γ (50 ng/ml), washed twice with 10 ml of ice-cold phosphate-buffered saline, and harvested with a Teflon cell scraper into an additional 10 ml of iced phosphate-buffered saline. Cell suspensions were centrifuged at 800 $\times$ *g* for 10 min, resuspended in 100 μl/75-cm^2 culture flask of ice-cold distilled H_2O containing a mixture of protease inhibitors (pepstatin 10 μg/ml, leupeptin 10 μg/ml, and phenylmethylsulfonyl fluoride 100 μM) and lysed by three cycles of freezing in liquid nitrogen and thawing in a 37 °C water bath. Lysates were centrifuged at 100,000 $\times$ *g* for 1 h, and supernatants were stored at −70 °C until use.

NOS Activity Measurement—NOS activity was measured in 96-well microtiter plates at 25 °C based on the kinetics of NADPH consumption or the oxidation of Fe^{2+}-myoglobin to Fe^{3+}-myoglobin, as described previously (14). For NADPH consumption measurements, incubation mixtures contained 50 mM Tris-HCl (pH 7.60), 100 μM $CaCl_2$, 10 μM tetrahydrobiopterin, 500 μM NADPH, 500 μM L-arginine, 1 mM DTT, 1 μM calmodulin, pH 7.6, and the indicated concentration of peptide in a final volume of 100 μl. Reactions were initiated by the addition of 20 pmol of nNOS, 10 pmol of eNOS, or 15 μg of rat iNOS-rich cytosol. NADPH consumption was determined from the rate of decrease in A_{340}, measured at 15-s intervals for a period of 30 min in a kinetic microplate spectrophotometer (Molecular Devices; Menlo Park, CA). The rate of decline in A_{340} measured when NOS was omitted from incubates was subtracted from all values. Samples in which iNOS activity was measured based on Fe^{2+}-myoglobin oxidation were prepared as above, but additionally contained 15 μg of rat iNOS-rich cytosol and a final concentration of 40 μM Fe^{2+}-myoglobin. Preparation of Fe^{2+}-myoglobin and spectrophotometric measurement of its rate of oxidation to Met-myoglobin by NO, was as described earlier (14).

^{125}I-Calmodulin Binding Measurement—Calmodulin was labeled with ^{125}I to a specific activity of 25–150 μCi/g, using the Bolton-Hunter method (15). ^{125}I-Calmodulin binding assays were performed in triplicate using 96-well microfiltration plates with GFB filter bottoms (Millipore, Bedford, MA). Before use, filters were preincubated for 1–2 min with 100 μl of buffer containing 50 mM Tris-HCl, pH 7.6, 1 mM DTT, 100 μM $CaCl_2$, and 0.5 mg/ml β-lactoglobulin; buffer was then removed by vacuum filtration. Binding reactions were comprised of: 50 mM Tris-HCl, pH 7.6, 1 mM DTT, 0.5 mg/ml β-lactoglobulin, 100 μM $CaCl_2$, 10 μM tetrahydrobiopterin, 1 nM ^{125}I-CaM (2500–5000 cpm) and 1–2 pmol of NOS in a 100-μl total volume. Samples were incubated for 15 min at 23 °C, and binding was quickly terminated by vacuum filtration. Filters were washed twice with 100 μl of ice-cold buffer containing 50 mM Tris-HCl, pH 7.6, and 100 μM $CaCl_2$ and air-dried. Scintillation mixture was added to each well (25 μl; OptiPhase SuperMix, Wallac Inc., Gaithersburg, MD), and plates were counted in a Microbeta Plus liquid scintillation counter (Wallac Inc.). Nonspecific binding was determined in samples that additionally contained 10 mM EGTA. In studies of the effect of inhibitory effect of peptide inhibitors on ^{125}I-CaM binding to NOS, blank binding was determined in the presence of peptide and absence of NOS. Dissociation of ^{125}I-CaM was similarly monitored in 96-well filtration plates. ^{125}I-CaM·nNOS complexes were first produced by incubation of 2 pmol of nNOS, 1 nM of ^{125}I-CaM, 100 μM $CaCl_2$, 10 μM tetrahydrobiopterin, 50 mM Tris-HCl, pH 7.6, 1 mM DTT, and 0.5 mg/ml β-lactoglobulin for 15 min (23 °C). To initate dissociation, a 3000-fold excess of unlabeled CaM (3 μM) was added at time 0, with or without simultaneous addition of the indicated concentration of bovine eNOS$^{607-634}$.

[^{3}H]N^GNitro-L-arginine Binding Measurement—Assays of [^{3}H]N^G-nitro-L-arginine binding were performed in 96-well polyvinylidene difluoride microfiltration plates (Millipore, Bedford, MA) as described previously (16), using 5 pmol of nNOS and the indicated concentrations of NOS-derived peptides.

Calcineurin Activity Measurement—Activity of the calmodulin-dependent phosphatase calcineurin (protein phosphatase 2B) was monitored in a 96-well kinetic microplate spectrophotometer at 37 °C, based on rate of hydrolysis of the artificial substrate *p*-nitrophenyl phosphate (17). Incubation mixtures contained 50 mM Tris-HCl, pH 7.6, 100 nM bovine brain calmodulin, 40 mM *p*-nitrophenyl phosphate, 400 μM $CaCl_2$, and 0.1% 2-mercaptoethanol in a 100-μl total volume. Reactions were initiated by the addition of 20 pmol of calcineurin, and activity was monitored continually at A_{405} for 60 min at 15-s intervals. Assay blanks additionally contained 10 mM EGTA, resulting in >90% inhibition of activity.

Proteolysis of NOS Isoforms—Limited proteolysis was performed on incubates containing 40 pmol of recombinant nNOS purified from stably transfected HEK-293 cells (11) or 50 pmol of recombinant eNOS purified from *E. coli* (12). Samples were preincubated at room temperature for 15 min in a 100-μl volume containing: 50 mM Tris, pH 7.6, 1 mM DTT, 10 μM CaM, 100 μM $CaCl_2$, with or without 10 mM EGTA. Proteolysis was initiated by the addition of 20 microunits of L-1-tosylamido-2-phenylethyl chloromethyl ketone-immobilized trypsin (Sigma) per pmol of NOS. Samples (25 μl) were collected after 0, 5, 10, and 20 min, and proteolysis was terminated by boiling with an equal volume of 2 $\times$ SDS gel-loading buffer. Peptide products were resolved on an 8–16% gradient SDS-polyacrylamide gel electrophoresis and visualized by staining with Coomassie Blue. Accurate molecular mass determination of tryptic fragments was performed by mass spectrometry at the Rockefeller University Protein/DNA Biotechnology Center, using matrix-assisted laser desorption and time of flight detection (Perseptive Biosystems Inc., Framingham, MA). For N-terminal sequence analysis, tryptic digests were prepared as above and subject to SDS-polyacrylamide gel electrophoresis, but then electrotransfered to polyvinylidene difluoride membranes. Amino acid sequencing was performed on an Applied Biosystems 477A protein sequencer.

Peptides—Synthetic peptides were obtained from SynPep (Dublin, CA) and other commercial suppliers. Purity was evaluated by high performance liquid chromatography and mass spectroscopy and exceeded 80% in all cases with typical purity ≈90%. Predominant impurities differed from the desired products by one amino acid residue, resulting from incompletely coupled synthesis.

Chemicals—Rat recombinant interferon-γ, RPMI culture medium, and cell culture reagents were from Life Technologies, Inc. Radioisotopes were from Dupont NEN, lipopolysaccharide (*E. coli* serotype 0111:B4), chemicals, and L-1-tosylamido-2-phenylethyl chloromethyl ketone-immobilized trypsin were obtained from Sigma, calmodulin was from Calbiochem, and tetrahydrobiopterin was from Schirks Laboratories (Jona, Switzerland). Enzymes were purchased from Pharmacia LKB Biotechnology, Promega, or New England Biolabs.

RESULTS AND DISCUSSION

Nitric oxide synthases are large multidomain enzymes in which a series of gene fusion events has resulted in the incorporation of modules showing significant homology to smaller ancestral proteins (18, 19). NOSs can be coarsely dissected into an N-terminal oxygenase domain and a C-terminal reductase domain, bridged by a canonical binding sequence for CaM (20). Calmodulin binding initiates electron transfer between the reductase and catalytic domains, thereby activating catalysis (21). The oxygenase domains have binding sites for substrate (arginine), heme, and tetrahydrobiopterin, whereas the reductase domain has binding sites for FAD, FMN, and NADPH.

Bredt *et al.* (22) were first to reveal the homology between the C-terminal half of NOS and NADPH-cytochrome P450 reductase (CPR), noting conserved regions corresponding to FMN, FAD, and NADPH binding domains. The FMN-binding modules of NOS isoforms and CPR are in turn highly homologous to the flavodoxins, which are small FMN-binding proteins that function as electron carriers in bacteria (23). The FAD and NADPH binding domains are closely related to chloroplast ferredoxin-$NADP^+$ reductase and other related proteins.

Sequence Alignments—Five flavodoxins have been crystallized and solved by x-ray diffraction (24). Three regions in these flavodoxins are involved in binding the FMN prosthetic group; the first of these is close to the N terminus, and is immediately proceeded by the initial β strand of the structure. Although only one of these FMN binding regions was identified in nNOS by Bredt *et al.* (22), each of them has a corresponding homolog

```
                                    INITIAL FMN BINDING REGION
NCPR_HUMAN  ESSFVEKMKK TGRNIIVFYG SQTGTAEEFA NRLSKD.AHR YGMRGMSADP  115
NOSE_BOVIN  GTLMAKRV.. ...KATILYA SETGRAQSYA QQLGRLFRKA FDPRVLCMD.  556
  NOSB_RAT  GQAMAKRV.. ...KATILYA TETGKSQAYA KTLCEIFKHA FDAKAMSME.  789
NOSM_MOUSE  RKVMASRV.. ...RATVLFA TETGKSEALA RDLATLFSYA FNTKVVCMD.  567
FLAV_ECOLI  .......... ..AITGIFFG SDTGNTENIA KMIQKQL.GK .D.VADVHDI   35
FLAV_DESVH  .......... .MPKALIVYG STTGNTEYTA ETIARELADA .GYEVDSRDA   38

                          FLANKING LOOP   SECOND FMN SITE
NCPR_HUMAN  EEYDLADLSS LPEIDNALVV FCMATYGEGD PTDNAQDFYD WL.QE.....  159
NOSE_BOVIN  .EYDVVSL.. ...EHETLVL VVTSTFGNGD PPENGESFAA AL.MEMSGPY  599
  NOSB_RAT  .EYDIVHL.. ...EHEALVL VVTSTFGNGD PPENGEKFGC AL.MEMRHP.  831
NOSM_MOUSE  .QYKASTL.. ...EEEQLLL VVTSTFGNGD CPSNGQTLKK SLFML.....  606
FLAV_ECOLI  AKSSKEDL.. ...EAYDILL LGIPTWYYGE ....AQCDWD DF.FP.....   70
FLAV_DESVH  ASVEAGGLF. ...EGFDLVL LGCSTWGDDS IE..LQDDFI PL.FD.....   76

                          LOCATION OF REGULATORY LOOP INSERT
NCPR_HUMAN  .......... .......... .......... ..........TDVDLSGVKF  169
NOSE_BOVIN  NSSPRPEQHK SYKIRFNSVS CSDPLVSSWR RKRKESSNTD SAGAGTLRFL  649
  NOSB_RAT  NS..VQEERK SYKVRFNSVS SYSDSRKSSG DGPDLRDNFE STGPLANVRF  879
NOSM_MOUSE  .......... .......... .......... .......... .RELNHTFRY  615
FLAV_ECOLI  .......... .......... .......... ........TL EEIDFNGKLV   82
FLAV_DESVH  .......... .......... .......... ........SL EETGAQGRKV   88

                          THIRD FMN SITE  FLANKING LOOP
NCPR_HUMAN  AVFGLGNKT. Y.EHFNAMGK YVDKRLEQLG AQRI  201
NOSE_BOVIN  CVFGLGSRA. Y.PHFCAFA. AVDTRLEELG GERL  680
  NOSB_RAT  SVFGLGSRA. Y.PHFCAFGH AVDTLLEELG GERI  911
NOSM_MOUSE  AVFGLGSSM. Y.PQFCAFAH DIDQKLSHLG ASQL  647
FLAV_ECOLI  ALFGCGDQED YAEYFCDALG TIRDIIEPRG ATIV  116
FLAV_DESVH  ACFGCGDSS. Y.EYFCGAVD AIEEKLKNLG AEIV  120
```

FIG. 1. **Structure-based sequence alignment of FMN binding domains of human NADP$^+$-cytochrome 450 reductase (*NCPR_HUMAN*), bovine eNOS (*NOSE_BOVIN*), rat nNOS (*NOSB_RAT*), mouse iNOS (*NOSM_MOUSE*) and flavodoxins from *E. coli* (*FLAV_ECOLI*), and *D. vulgaris* (*FLAV_DESVH*).** Complete sequences were obtained from the Swiss Protein data base using the given designations. Alignment was performed manually by aligning the flavin binding sequences and conserved secondary structural elements from flavodoxin crystal structures as evaluated with Biosym's Homology software. The C-terminal end of the domain (≈35 residues for *Desulfovibrio* sequence) is omitted to conserve space.

in NOSs. The first step in alignment of the NOS FMN binding domain with the flavodoxins was the identification of these regions in each NOS isoform. This was followed by the identification of conserved secondary structural elements in NOS, primarily by their homology to the corresponding elements in flavodoxins by mutation matrix criteria (10).

Fig. 1 shows alignment of a select set of NOS, CPR, and bacterial flavodoxin sequences, illustrating the conservation of regions involved in FMN binding. It is obvious that a major insertion of ≈45 amino acids has occurred in mammalian cNOSs. A corresponding insert is also found in the FMN binding region of the cloned invertebrate cNOSs from *Rhodnius prolixus* (25) and *Drosophila melanogaster* (26); these inserts are somewhat larger (54–63 amino acids), but contain regions of marked homology to mammalian cNOS inserts. Expanding this alignment to include dozens of known flavodoxins and related FMN-containing flavoproteins reveals that only cNOSs exhibit such an insertion. Moreover, the corresponding region of iNOS sequences closely resemble flavodoxin sequences but lack an insert anywhere within the FMN binding domain. Therefore, occurrence of the amino acid insertion correlates with Ca^{2+}/CaM control. This insertion represents the single most prominent difference between cNOSs and iNOS amino acid sequences, considered over their entire length.

The cNOS FMN module insertions are notably rich in charged residues and have an excess of positive charge. This is especially true of the eNOS isoform, which contains the motif RRKRK. Considerable homology exists between the cNOS insertions, particularly toward their N termini. It is also apparent that some structural reorganization has taken place during evolution, which may allow the two or three positively charged residues (depending on species) in the nNOS equivalent of the RRKRK region to recognize a similar binding site. The pattern of conservation suggests that eNOS and nNOS insertions contain at least two motifs.

Structural Models—The availability of solved x-ray crystal structures for flavodoxins allows us to position the insertion in three dimensions relative to the calmodulin binding site. Homology-based molecular models have been constructed for the FMN binding domains of cNOSs, iNOS, and CPR, which could be relaxed to a sterically and energetically reasonable state. After relaxation of these FMN binding domain models, no steric overlaps were present, and energies were approximately −300 kcal, comparable or lower than that of reference flavodoxin crystal structures.

As shown in Fig. 2 (*upper left*), the backbone structure of iNOS and CPR are virtually superimposable on the backbone of *Desulfovibrio vulgaris* flavodoxin, the closest solved structural homolog of the FMN binding modules of the NOS isoforms.[2] The structure, a Rossmann fold motif (28), is a five stranded parallel β-sheet with the FMN binding site along one edge. Homology predicts that two aromatic residues in murine iNOS, Phe^{587} and Tyr^{625}, are in contact with the FMN ring system; Tyr^{625} serves as a shielding residue.

Fig. 2 (*upper right*) shows the corresponding backbone structure of eNOS; nNOS is extremely similar but not shown. Most of the eNOS backbone can be superimposed on homologs shown in Fig. 2 (*upper left*), with the insertion projecting from the upper edge of the sheet opposite the FMN binding site. Structurally, it corresponds to the replacement of a tight 5–10 residue $\alpha \rightarrow \beta$ loop with an ≈50-residue structure about one-third the size of the entire FMN binding module. We are unable to propose a conformation for the insertion because we lack a solved homolog; the structure shown is merely intended to convey relative position and size.

The CaM binding site is immediately adjacent to the N-terminal edge of the FMN binding domain (painted *white* in Fig. 2, *upper left*). With CaM bound, the CaM recognition site would predictably be in a helical conformation (29, 30); steric constraints suggest that it extends almost directly away from the FMN binding domain. The *lower panels* of Fig. 2 show models of the FMN binding domains of iNOS (*left*) and eNOS (*right*) with CaM (*yellow* ribbon; based on Vorherr *et al.* (30)) positioned above the N-terminal strand of the FMN domain. There are 7–8 residues between the end of the CAM recognition site proper and the start of the initial strand of the β-sheet; 2–3 residues at each end of this short linker are needed to clear the van der Waals surfaces of CaM and the FMN domain. This leaves 2–3 residues that are conformationally unrestricted, and, hence, there are uncertainties about the exact position above the β-sheet of CaM and the orientation of the axis of the CaM recognition site. The position of CaM relative to the FMN domain is unspecified with respect to rotations about the *y* axis of Fig. 2 by available information (corresponding to the axis of

[2] Recently, the crystal structure of NADPH-cytochrome P450 oxidoreductase has been reported at 3.0 Å resolution (27). The FMN-binding module bears striking homology to *D. vulgaris* flavodoxin.

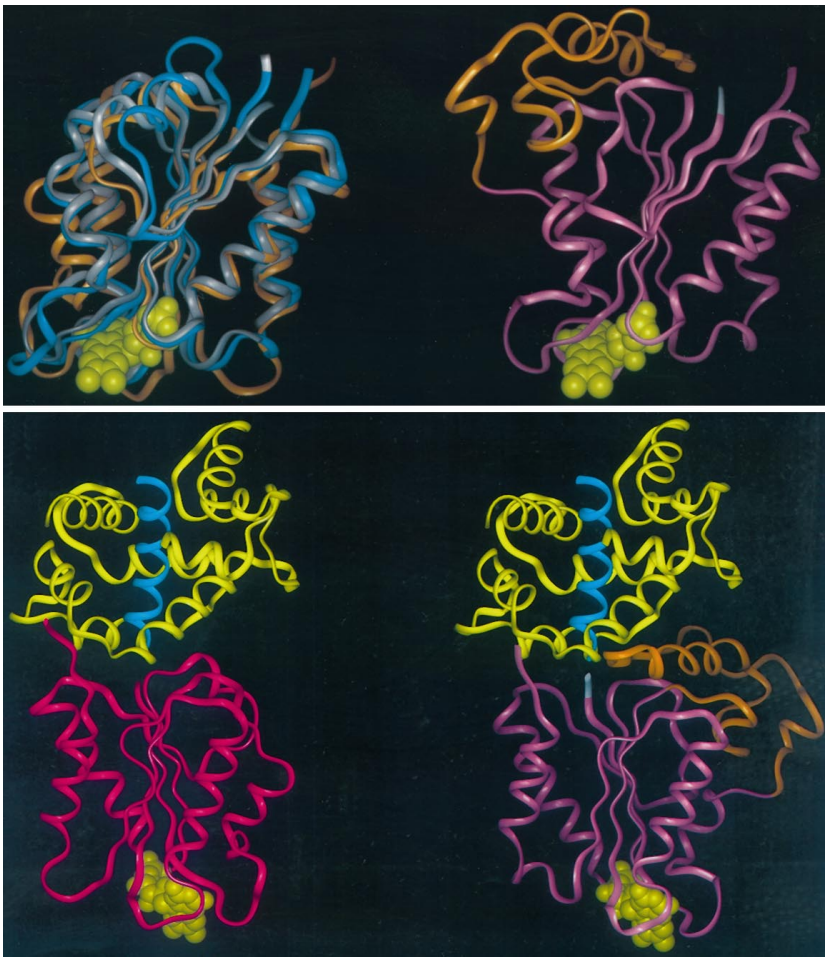

FIG. 2. **Structural models of FMN binding domains.** *Upper left panel*, flavodoxin (*silver*; from McMillan *et al.* (11)), cytochrome P450 reductase (*gold*; homology model), rat iNOS (*cyan*, homology model). *Upper right panel*, bovine eNOS (*pink*, with autoinhibitory peptide in *gold*; homology model). N-terminal residues of NOS isoform domains are depicted in *white* with the CaM binding site directly above this point. FMN is shown in space filling representation at *bottom*. Central β-sheets and flanking α-helices are visible in all structures. *Lower panels*, approximate location of bound CaM (*yellow*, with NOS CaM binding sequence in *blue*) relative to FMN binding domain (*pink*, with FMN in *gold* space-filling rendering) of rat iNOS (*left*) and bovine eNOS (*right*).

the CaM-binding helix of *lower panels*). It is notable that calmodulins (molecular mass $\approx$ 17 kDa) are larger than the entire FMN-binding module. Although the insertion is midway through the sequence of the FMN-binding module, in three dimensions the model predicts it to be directly adjacent to the CaM binding site. The model predicts also that CaM binding would be sterically hindered by the insertion, suggesting that the insertion can exist in more than one physiologically relevant conformation.

Two aspects of this model strongly suggest that the insert functions as a control element, 1) the correlation between Ca^{2+}/CaM control and the presence of the insertion and 2) the proximity of the CaM binding site to the insertion and the probable steric interactions which would ensue. An attractive potential role for the insert is that of an inhibitory polypeptide which is displaced by CaM binding. It differs from inhibitory polypeptides common to other CaM-dependent enzymes, and CaM itself, in its lack of acidic and hydrophobic amino acids; this makes direct binding of the insertion to CaM sites in NOS isoforms unlikely. Nonetheless, CaM could conceivably displace the polypeptide insert from a neighboring site by binding domain overlap or through allosteric effects.

Synthetic Polypeptide Effects on NOS Activity—Functional significance of the putative autoinhibitory insert of cNOSs was evaluated using a series of synthetic polypeptide fragments. Polypeptides corresponding to promising recognition sites such as the RRKRK motif of the eNOS insert were synthesized in lengths ranging from 6 to 33 residues, as shown in Table I. Both eNOS- and nNOS-derived peptide fragments were evaluated; effects on NOS activity are summarized in Table II. At concentrations of 50–100 μM, several polypeptide fragments of the cNOS insertions profoundly inhibited eNOS and nNOS activity. The most effective inhibitory polypeptides were from the eNOS insertion and contained the RRKRK motif (Table II and Fig. 3*A*). Human nNOS-derived polypeptides weakly inhibited eNOS, but were without effect on nNOS. While all peptides were less potent on iNOS, significant inhibition was obtained with $eNOS^{601–633}$ and $eNOS^{607–634}$. Notably, inhibition of iNOS activity by these peptides was rapid and apparently complete within one minute of addition. Because CaM is very tightly bound to iNOS and has a remarkably slow off-rate, with little dissociation occurring even after boiling (5), inhibition probably occurs without CaM displacement.

Synthetic Polypeptide Effects on Calmodulin Binding—Overlap of the cNOS polypeptide insert and the CaM recognition site, suggested from molecular modeling, implies that the insert may obstruct CaM binding. If this involves "docking" of the insert within cNOSs, synthetic homologs of the insert might similarly bind and interfere with CaM binding. As shown in Table II, potent inhibition of ^{125}I-CaM binding to nNOS was observed with insert-derived polypeptide fragments; relative peptide potency for inhibiting CaM binding mirrored that for blocking nNOS activation. IC_{50} values for eNOS-derived peptide fragments ranged from 1 to 10 μM, and potency increased as the RRKRK motif was progressively lengthened to include up to 33 amino acids (Fig. 3*B*). Inhibition of nNOS activity and CaM binding by insert-derived peptides was fully reversed by excess CaM (see Fig. 3, *C* and *D*, for findings with $eNOS^{607–634}$), indicative of a competitive mode of inhibition. Thus, the greater apparent potency of peptides for inhibiting CaM binding *versus* activity, indicated in Table II, is explained by differences in assay conditions; lower CaM concentrations

were used to assess binding (1 nM) *versus* activity (100 nM). Inhibition of CaM binding by peptide could not be overcome by excess Ca^{2+} (Fig. 3*E*).

Conceivably, the synthetic peptides could interfere with CaM binding to NOS by interacting with either NOS or CaM itself. That NOS is the actual binding target for eNOS-derived insert peptides is indicated by several findings. First, direct binding of peptide to ^{125}I-CaM, quantified in the absence of NOS, was undetectable at concentrations that inhibited >90% of CaM binding to nNOS (data not shown). Second, the CaM-dependent phosphatase calcineurin, which resembles cNOSs in having a K_d for CaM of 5 nM (31), was not inhibited by concentrations of insert-derived peptides that potently inhibit nNOS activity (see Fig. 4). Third, eNOS-derived peptides markedly enhanced the dissociation rate of ^{125}I-CaM from preformed complexes with nNOS (Fig. 3*D*). In this experimental setting, dissociated ^{125}I-CaM is prevented from reassociating with NOS by addition of a 3,000-fold molar excess of unlabeled CaM. Thus, in order for a synthetic eNOS-derived peptide to *eject* CaM from its binding site on nNOS, it must at least transiently form a ternary CaM-containing complex with NOS. Conceivably, this transient ternary complex could involve interactions of peptide with CaM as well as NOS. These findings suggest that the binding domain of the putative eNOS autoinhibitory element on nNOS either overlaps or allosterically perturbs the CaM binding domain.

Previously described inhibitors with demonstrated selectivity for NOS influence the arginine site in a manner that can be detected as a loss in sites or binding affinity for the arginine analog, [^{3}H]N^G-nitro-L-arginine. Thus, it is notable that the cNOS insert peptides inhibit NOS activity and CaM binding with a slight increase, rather than decrease, in [^{3}H]N^G-nitro-L-arginine binding (Table II). Specificity of the insert peptides is also indicated by a lack of inhibition of either NOS activity or CaM binding with each of five synthetic peptides, 10–15 amino acids in length, derived from sites on the FMN binding domain of cNOSs, which are distinct from the insert polypeptide (not shown).

Effects of Calmodulin on Exposure of the Insert—Displacement of the insert peptide from an internalized binding site on cNOSs by CaM would conceivably enhance exposure of the insert to proteolysis. This hypothesis was tested by examining the pattern of peptide accumulation during limited trypsinolysis of both nNOS and eNOS, in the absence and presence of bound CaM (Fig. 5).

Earlier, Sheta *et al.* (20) showed that of 165 possible tryptic cleavage sites in rat nNOS, a single preferred cut site resides at Arg^{727} within the CaM binding sequence. Cutting at this site has served as an effective means for isolation of distinct reductase and oxygenase domains. With CaM present but not bound (due to addition of the Ca^{2+}-chelator, EDTA; see Fig. 5*A*), we similarly observe that tryptic cleavage of nNOS occurs almost exclusively at a single site, consistent with Arg^{727} within the CaM binding site. Accordingly, we found a time-dependent accumulation of fragments with apparent molecular masses of 77 and 85 kDa, corresponding to C-terminal reductase and N-terminal oxygenase domains, respectively (Fig. 5*A*). When CaM was permitted to bind nNOS, by omission of EDTA, Arg^{727} was protected from proteolysis, and a novel tryptic cleavage site was revealed. Cutting at this new site yielded fragments of apparent molecular masses of 63 and 93 kDa (Fig. 5*A*). Molecular mass refinement by matrix-assisted laser desorption ionization spectrometry indicated the smaller fragment to be 64,809 ± 324 Da. This product is best explained by cleavage at Arg^{855}–Lys^{856}, a dibasic (RK) site within the insert peptide which predicts a C-terminal fragment of 65,071 Da. That this fragment originates from the C terminus of nNOS is indicated by our finding that it is the predominant trypsinolysis product of the bacterial-expressed C-terminal reductase domain (nNOS$^{721–1429}$) but is not produced by trypsinolysis of the N-terminal oxygenase domain (nNOS$^{1–721}$) (data not shown). Confirmation of cleavage at Lys^{856} is provided by direct sequence analysis of its 10 N-terminal amino acids (KSSGDGPDLR). In accord with our findings, a thorough analysis of nNOS trypsinolysis, in the absence of bound CaM, indicates that Lys^{856} becomes a cut site following initial cleavage within the CaM binding site at Arg^{727} (32). Since Lys^{856} is protected from tryptic cleavage in the absence of CaM, but exposed when CaM is bound (or the CaM binding site is severed), we conclude that CaM displaces the FMN domain insert peptide of nNOS.

A similar conclusion is drawn from study of eNOS fragmentation after limited trypsinolysis. When CaM is not bound, tryptic cleavage of eNOS yields four principal peptides of nominal molecular masses of 57, 60, 68, and 77 kDa (Fig. 5*B*). This pattern is rationalized by cleavage at Arg^{518} within the CaM

TABLE I
Peptide derivation and composition

Sequence and derivation of polypeptides excerpted from the insert in the FMN binding domain of cNOSs and tested for effects on NOS activity and binding.

Designation	Derivation[a]	Sequence
eNOS$_{628–633}$	b	WRRKRK
eNOS$_{626–636}$	b	SSWRRKRKESS
nNOS$_{835–845}$	h	QEERKSYKVRF
eNOS$_{604–615}$	h	RPEQHKSYKIRF
eNOS$_{601–633}$	b	SSPRPEQHKSYKIRFNSVSCSDPLVSSWRRKRK
eNOS$_{607–634}$	b	QHKSYKIRFNSVSCSDPLVSSWRRKRKE
nNOS$_{851–864}$	r	SDSRKSSGDGPDLR
nNOS$_{835–864}$	h	QEERKSYKVRFNSVSSYSDSQKSSGDGPDL

[a] h, human; b, bovine, r, rat.

TABLE II
The FMN binding domain insert of cNOSs: effect of peptide fragments on NOS activity and ligand binding

Peptide		NOS activity[a]			Ligand Binding to nNOS[b]	
		nNOS	eNOS	iNOS	[^{3}H]-NNA	^{125}I-CaM
	μg/ml (μM)			*% of control*		
eNOS$_{628–633}$	100 (107.0)	11.0 ± 3.3	24.0 ± 2.8	91.1 ± 5.7	91.7 ± 5.1	6.7 ± 3.6
eNOS$_{626–636}$	100 (71.2)	19.1 ± 0.9	27.7 ± 2.0	92.1 ± 1.3	120.7 ± 12.7	0.0 ± 0.5
nNOS$_{835–845}$	100 (68.1)	102.0 ± 2.1	93.6 ± 2.3	101.1 ± 3.7	118.9 ± 4.1	82.7 ± 1.1
eNOS$_{604–615}$	100 (63.0)	54.5 ± 1.8	80.5 ± 2.0	99.7 ± 5.7	115.0 ± 8.6	24.7 ± 2.2
eNOS$_{601–633}$	300 (76.0)	30.4 ± 1.7	57.2 ± 7.5	62.2 ± 2.8	116.3 ± 1.9	0.0 ± 7.4
eNOS$_{607–634}$	300 (87.7)	28.2 ± 0.9	40.2 ± 4.0	64.3 ± 3.2	122.4 ± 1.0	0.0 ± 4.8
nNOS$_{851–864}$	100 (72.0)	98.4 ± 1.9	102.6 ± 4.1	99.7 ± 2.8	119.2 ± 3.4	89.2 ± 6.2
nNOS$_{835–864}$	300 (84.8)	103.0 ± 1.3	80.2 ± 3.8	84.1 ± 3.5	95.7 ± 4.7	82.7 ± 1.1

[a] NOS activity measurements were performed using purified recombinant nNOS and eNOS, or native iNOS. Values are means ± S.E. of triplicate determinations.

[b] Radioligand binding was performed after incubation of 1–2 pmol of NOS for 15 min at 23 °C with either ^{125}I-calmodulin (1 nM) or [^{3}H]N^G-nitro-L-arginine (NNA) (200 pM) and the indicated peptides. Values are means ± S.E. of triplicate determinations.

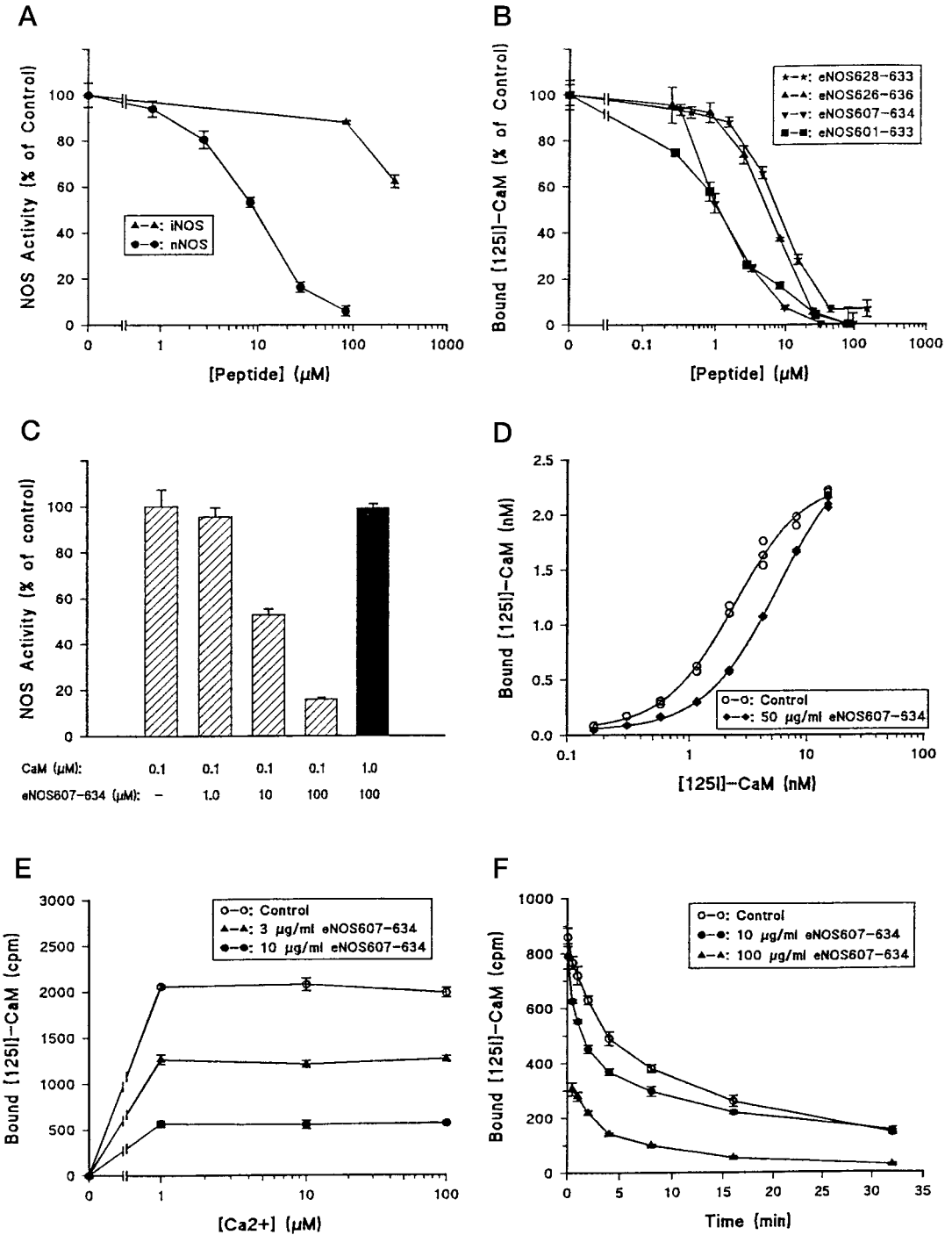

FIG. 3. **Influence of eNOS-insert peptides on NOS activity and CaM binding.** *Panel A*, NOS activity is inhibited by $eNOS^{601–633}$. nNOS activity was measured kinetically, based on the rate of NADPH consumption; iNOS activity was measured as the rate of NO formation, based on Fe^{2+}-myoglobin oxidation. Activities are expressed as percent of control samples in which $eNOS^{601–633}$ was omitted. *Panel B*, ^{125}I-CaM binding to nNOS is inhibited by eNOS insert-derived peptides. Specific inhibition of ^{125}I-CaM binding to nNOS was assessed as a function of concentration of added peptide in a 96-well microfiltration plate assay. *Panel C*, Inhibition of nNOS activity by $eNOS^{607–634}$ is reversed by excess CaM. Activity was measured as percent NADPH consumption rate in the presence of a maximally effective concentration of CaM (0.1 mM), prior to addition of peptide. Note that inhibition of nNOS activity was greater than 80% after addition of 100 mM $eNOS^{607–634}$, but restored to the control level by addition of 10-fold more CaM (*solid bar*). *Panel D*, Inhibition of ^{125}I-CaM binding to nNOS by $eNOS^{607–634}$ is competitive with [CaM]. ^{125}I-CaM binding assays were performed as for *panel B*, over a range of CaM concentrations in the absence (*control*) or presence of peptide. *Panel E*, inhibition of CaM binding to nNOS by $eNOS^{607–634}$ is not reversed by Ca^{2+} excess. ^{125}I-CaM binding assays were performed as for *panel B*, except that $CaCl_2$ concentrations were varied. "Zero" Ca^{2+} (<1 nM) was achieved by inclusion of 10 mM EGTA. *Panel F*, dissociation of ^{125}I-CaM from nNOS is accelerated by $eNOS^{607–634}$.

binding site ($eNOS^{1–518}$ = 56,877 Da, $eNOS^{519–1204}$ = 76,308 Da) and at a second site, likely to be Lys^{545}, which resides between the CaM binding site and insert peptide ($eNOS^{1–545}$ = 59,916; $eNOS^{546–1204}$ = 73,270). Exposure of Lys^{545} and proximity to the CaM binding site is predicted in the model shown in Fig. 2; this site appears to be within a helix-turn transition at the edge of the β-sheet distant from the FMN binding site. Lack of cleavage in nNOS at the site homologous to eNOS Lys^{545} may be explained by the presence of a single basic residue, while eNOS contains paired basic residues (RK). In

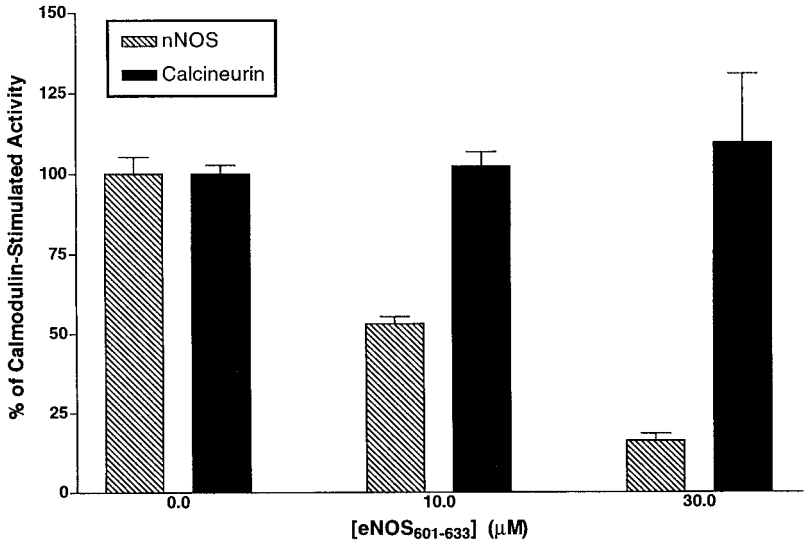

FIG. 4. **CaM-stimulated nNOS activity, but not calcineurin activity, is inhibited by the FMN insert-derived peptide eNOS$_{607-633}$.** Kinetic assays were performed as described under "Experimental Procedures"; *bars* represent means of triplicate determinations ± S.E., performed in the absence and presence of the indicated peptide concentrations. Reaction blanks were performed in the presence of 10 mM EGTA to define CaM-dependent activity of nNOS and calcineurin. In both cases, EGTA reduced activity to a level >10% of that measured in the absence of calcium chelator.

any event, binding of CaM simplifies this cleavage pattern by providing a single dominant cut site. Neglecting the intact proteins and the 10-kDa band from small unresolved fragments of eNOS, only two strong bands are visible at 60 and 65 kDa. These are predicted by cleavage of the molecule within the pentabasic RRKRK motif in the insert peptide at residue Lys^{632}. Thus, cleavage at Lys^{632} (with additional cleavage of the N-terminal fragment at Lys^{545}) produces fragments of 59,916 Da (eNOS$^{1-545}$) and 63,251 Da (eNOS$^{633-1024}$). Alignment reveals close correspondence between Lys^{632} of eNOS and Lys^{856} of nNOS (see Fig. 1), suggesting that CaM binding similarly displaces the insert peptide in each cNOS isoform.

To summarize, CaM binding not only protects the CaM binding site from degradation by trypsin, but exposes cleavage sites on both nNOS and eNOS, which are otherwise inaccessible. A preponderance of evidence points to the clusters of basic residues in the FMN domain insert as the trypsin cleavage sites which are exposed by CaM binding. Exposure of cryptic sites by CaM binding could occur by an allosteric mechanism, or by displacement through binding domain overlap. CaM-driven movement of the insert strongly suggests a switch function for activation of NO synthesis.

Mechanism of NOS Control—Herein we have shown that cNOSs possess a polypeptide insert in their FMN binding modules that is 1) unique to NOS isoforms which are regulated by transient CaM binding; 2) positioned adjacent to the CaM binding domain; 3) an impediment to CaM binding and hence, NOS activation; and 4) displaced when CaM binding *does* occur. Together, these results strongly imply that the insertion in cNOSs is an autoinhibitory control element. We propose that inhibition of NOS by the insert requires occupancy of key sites on cNOS. CaM binding displaces the insert, thus activating cNOS catalysis by "disinhibition." Close proximity of the inhibitory polypeptide to its cognate binding site(s) on cNOSs would result in an exceedingly high local concentration, thus favoring the bound/inhibited state in the absence of CaM. The detection of basal activity with either purified eNOS or nNOS, in the simultaneous presence of EGTA and absence of CaM (≈5% of maximal),[3,4] may arise from a low steady-state concentration of the disinhibited cNOS conformer.

The control mechanism requires that CaM displace the insert upon binding to cNOS; this should translate into a reduced affinity for CaM. Reciprocally, absence of the insert from iNOS would preclude the otherwise expected steric hindrance to CaM binding, contributing to the much tighter binding of CaM at low levels of Ca^{2+}. Studies of polypeptides, corresponding to the putative CaM binding sites on eNOS and iNOS, and of chimeras in which the putative CaM binding sequence of one NOS isoform is substituted with the corresponding portion of another, have indicated that affinity and calcium-dependence of CaM binding is provided by elements on NOS in addition to the recognized CaM binding sequence itself (6, 7). These results have been interpreted as indicating the presence of an auxiliary CaM binding region on iNOS that augments binding. An alternative explanation, raised by our findings, is that the absence of the autoinhibitory polypeptide from iNOS contributes to enhanced CaM affinity at low Ca^{2+} levels. We hypothesize that iNOS evolved from an ancestral cNOS-like protein by loss of the inhibitory peptide; nonetheless, vestigial regulatory sites are suggested by a weak inhibition of activity in the presence of synthetic fragments of the eNOS inhibitory peptide. The CaM binding sites on iNOS and cNOS are apparently related to a similar basic region near the N terminus of CPR, and may have evolved from such a region in a common ancestral protein.

Our data suggest that binding of the inhibitory peptide may involve at least two regions. At least one recognition site binds the RRKRK motif. A second possible site might recognize sequences such as EERKSYKVRF and EQHKSYKIRF that occur in the N-terminal half of the eNOS and nNOS insertions; peptides that lack RRKRK but contain these sequences weakly inhibit NOS activity and CaM binding. Some similarity between the first and second halves of the insertion can be readily noted by comparing the sequences of peptide eNOS$^{628-633}$ and eNOS$^{626-636}$ with those of nNOS$^{835-845}$ and eNOS $^{604-615}$. The insert peptide also contains an abundance of serine and threonine residues which provide potential sites for phosphorylation (12/45 residues in the bovine eNOS insert). We speculate that phosphorylation/dephosphorylation may influence the affinity of insert peptides for binding cognate sites on cNOSs and hence, impact on parameters of NOS activation and/or deactivation. In this regard, it is notable that skeletal muscle possesses an nNOS splice variant in which the insert peptide is expanded by 36 residues (33), providing additional sites for possible cell-type specific modification.

Many important questions remain to be answered. The location and identity of the sites of interaction with the inhibitory polypeptide on the surface of the enzyme are not known. Regions of interaction could include the flanking surface loops of

[3] Q. Liu and S. Gross, unpublished observation.
[4] P. Martasek and B. S. S. Masters, unpublished observation.

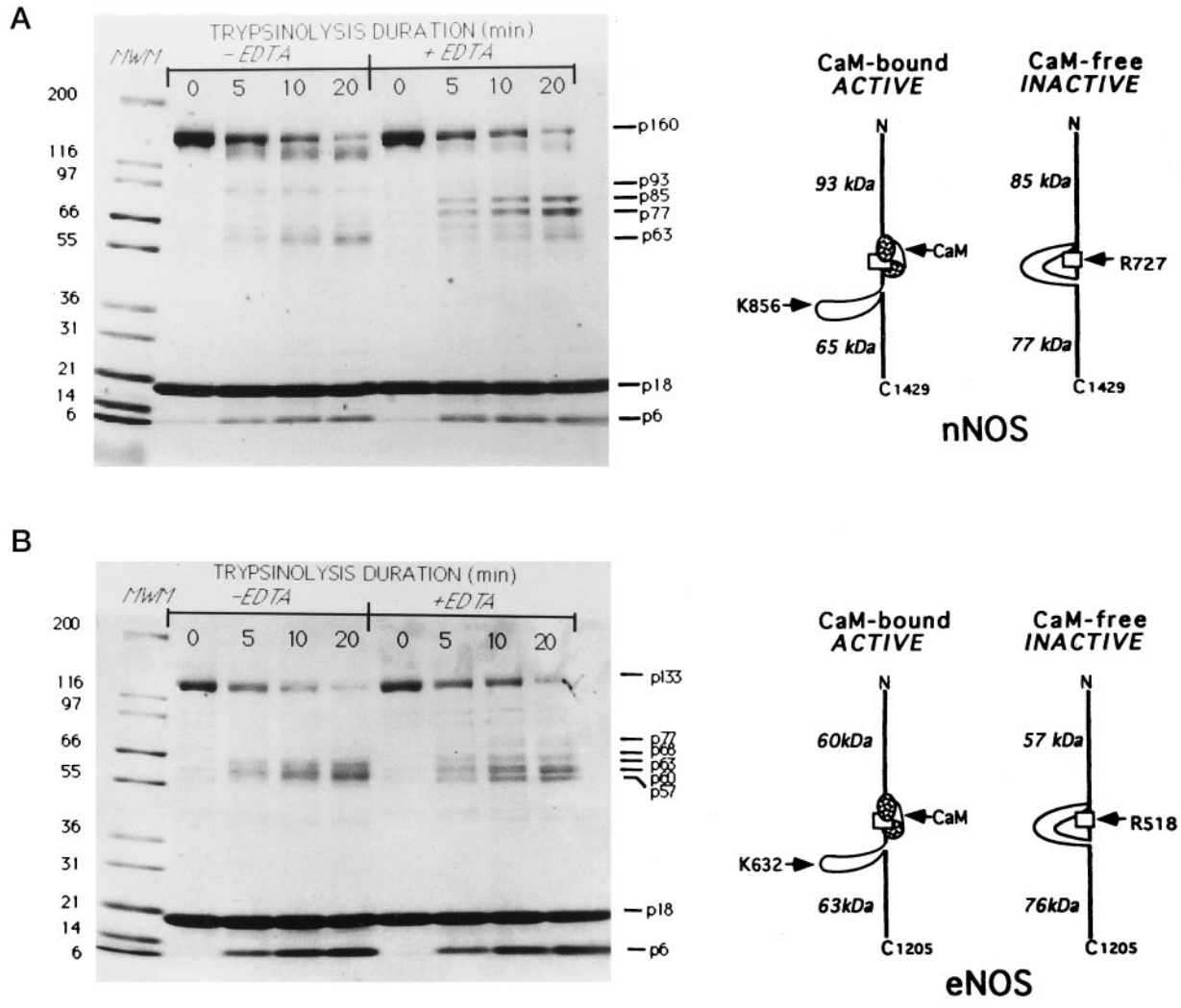

FIG. 5. **SDS-polyacrylamide gel electrophoresis showing the products of limited tryptic digestion of cNOSs.** Trypsinolysis of nNOS (*panel A*) and eNOS (*panel B*) was performed for the indicated duration in the absence (+*EDTA*) or presence (−*EDTA*) of bound CaM. Protein bands at 160, 133, and 17 kDa correspond to uncut nNOS, eNOS, and CaM, respectively. Results indicate that a preferred tryptic cleavage site resides within the CaM binding sequence of cNOSs, however, when this site is masked by bound CaM, a novel tryptic cleavage is revealed within the FMN domain polypeptide insert. *Panel A* shows the progressive formation from nNOS of 75- and 85-kDa fragments in the absence of bound CaM (*lanes 2–5*), and the accumulation of two alternative fragments of 63 and 93 kDa when CaM is bound (*lanes 6–9*). *Panel B* shows the corresponding experiment with eNOS giving a more complicated tryptic cleavage pattern in the absence of bound CaM (*lane 6–9*) that is simplified to two major fragments of 60 and 65 kDa when CaM is bound (*lanes 2–5*). See text for detailed interpretation of cleavage sites.

the FMN domain, bound CaM, and additional more distant sites. In particular, a site on the oxygenase domain consisting of an array of acidic groups could serve as a binding site for the basic regions on the inhibitory polypeptide insert which stabilizes the inhibited conformation of cNOS.

While it seems clear that CaM binding and activation of cNOS is associated with displacement of the inhibitory polypeptide, it is not known how the presence of the polypeptide in its initial conformation inhibits electron transfer. An obvious mechanism would involve interference by the inhibitory polypeptide with interactions between the oxygenase and reductase domains or flavin subdomains, stabilizing a conformation which does not support rapid electron transfer. Such interference could involve changes in either heme/FMN or FMN/FAD distances driven by domain realignment. Intramolecular electron transfer rates are often determined by the ability of electrons to tunnel, and therefore fall off exponentially with distance at roughly an order of magnitude per bond length (34); thus, a small increase in interdomain distance could produce a large reduction in electron flux. Displacement of the inhibitory peptide may not be the only mechanism by which CaM binding stabilizes the activate conformation of cNOSs, inasmuch as CaM removal results in inactivation of iNOS.

In conclusion, we have identified a novel control element in cNOSs which will serve as a prototype for the development of potent peptide inhibitors. The exposure of tryptic cleavage sites in this element represents the first demonstration of a specific CaM-induced conformational change in NOS and may be a hallmark of the active conformer of NOS. Abu-Soud and Stuehr (21) pointed out that the use of CaM to control electron transfer is unique to cNOS. A more fundamental difference between cNOS and other CaM-regulated proteins is the lack of a CaM analog within the cNOS inhibitory peptide. Ultimately, cNOS may not be unique in this regard; it may presage the identification of other CaM regulated systems in which the CaM/inhibitor interaction is mediated through binding domain overlap or allosteric effects, rather than competition for a common recognition site.

Acknowledgments—The encouragement and support of Joe DeAngelo and APEX Biosciences Inc. are responsible for the pilot studies that brought this investigation to fruition.

REFERENCES

1. Nathan, C., and Xie, Q. W. (1994) *Cell* **78,** 915–918
2. Ignarro, L. J. (1990) *Annu. Rev. Pharmacol. Toxicol.* **30,** 535–560
3. Moncada, S., Palmer, R. M., and Higgs, E. A. (1989) *Biochem. Pharmacol.* **38,** 1709–1715
4. Nathan, C., and Xie, Q. W. (1994) *J. Biol. Chem.* **269,** 13725–13728
5. Cho, H. J., Xie, Q. W., Calaycay, J., Mumford, R. A., Swiderek, K. M., Lee, T. D., and Nathan, C. (1992) *J. Exp. Med.* **176,** 599–604
6. Venema, R. C., Sayegh, H. S., Kent, J. D., and Harrison, D. G. (1996) *J. Biol. Chem.* **271,** 6435–6440
7. Ruan, J., Xie, Q., Hutchinson, N., Cho, H., Wolfe, G. C., and Nathan, C. (1996) *J. Biol. Chem.* **271,** 22679–22686
8. Jarrett, H. W., and Madhavan, R. (1991) *J. Biol. Chem.* **266,** 362–371
9. Brickey, D. A., Bann, J. G., Fong, Y. L., Perrino, L., Brennan, R. G., and Soderling, T. R. (1994) *J. Biol. Chem.* **269,** 29047–29054
10. Dayhoff, M. O., Hunt, W. C., and Hunt, L. T. (1983) *Methods Enzymol.* **91,** 524–545
11. McMillan, K., Bredt, D. S., Hirsch, D. J., Snyder, S. H., Clark, J. E., and Masters, B. S. (1992) *Proc. Natl. Acad. Sci. U. S. A.* **89,** 11141–11145
12. Martasek, P., Liu, Q., Liu, J., Roman, L. J., Gross, S. S., Sessa, W. C., and Masters, B. S. (1996) *Biochem. Biophys. Res. Commun.* **219,** 359–365
13. Gross, S. S., and Levi, R. (1992) *J. Biol. Chem.* **267,** 25722–25729
14. Gross, S. S. (1996) *Methods Enzymol.* **268,** 159–168
15. Bolton, A. E., and Hunter, W. M. (1973) *Biochem. J.* **133,** 529–539
16. Nishimura, J. S., Martasek, P., McMillan, K., Salerno, J., Liu, Q., Gross, S. S., and Masters, B. S. (1995) *Biochem. Biophys. Res. Commun.* **210,** 288–294
17. Takai, A., and Mieskes, G. (1991) *Biochem. J.* **275,** 233–239
18. Masters, B. S., McMillan, K., Sheta, E. A., Nishimura, J. S., Roman, L. J., and Martasek, P. (1996) *FASEB J.* **10,** 552–558
19. Liu, Q., and Gross, S. S. (1996) *Methods Enzymol.* **268,** 311–324
20. Sheta, E. A., McMillan, K., and Masters, B. S. (1994) *J. Biol. Chem.* **269,** 15147–15153
21. Abu-Soud, H. M., and Stuehr, D. J. (1993) *Proc. Natl. Acad. Sci. U. S. A.* **90,** 10769–10772
22. Bredt, D. S., Hwang, P. M., Glatt, C. E., Lowenstein, C., Reed, R. R., and Snyder, S. H. (1991) *Nature* **351,** 714–718
23. Porter, T. D. (1991) *Trends Biochem. Sci.* **16,** 154–158
24. Watenpaugh, K. D., Sieker, L. C., and Jensen, L. H. (1973) *Proc. Natl. Acad. Sci. U. S. A.* **70,** 3857–3860
25. Yuda, M. (1996) GenBank™ accession no. U59389
26. Regulski, M., and Tully, T. (1995) *Proc. Natl. Acad. Sci. U. S. A.* **92,** 9072–9076
27. Kim, J.-J., Wang, M., Roberts, D. L., Paschke, R., Shea, T., and Masters, B. S. S. (1996) in *Flavins and Flavoproteins* (Stevenson, K. J., ed) pp. 455–462, University of Calgary Press, Calgary, Alberta, Canada
28. Rossmann, M. G., Moras, D., and Olsen, K. W. (1974) *Nature* **250,** 194–199
29. O'Neil, K. T., and De Grado, W. F. (1990) *Trends Biochem. Sci.* **15,** 59–64
30. Vorherr, T., Knopfel, L., Hofmann, F., Mollner, S., Pfeuffer, T., and Carafoli, E. (1993) *Biochemistry* **32,** 6081–6088
31. Imparl, J. M., Senshu, T., and Graves, D. J. (1995) *Arch. Biochem. Biophys.* **318,** 370–377
32. Lowe, P. N., Smith, D., Stammers, D. K., Riveros-Moreno, V., Moncada, S., Charles, I., and Boyhan, A. (1996) *Biochem. J.* **314,** 55–62
33. Silvagno, F., Xia, H., and Bredt, D. S. (1996) *J. Biol. Chem.* **271,** 11204–11208
34. Moser, C. C., Keske, J. M., Warncke, K., Farid, R. S., and Dutton, P. L. (1992) *Nature* **355,** 796–802